

# An investigation of the influence of cold-rolling on the structure factor of a metallic glass

WU GUOAN\*, N. COWLAM

*Department of Physics, University of Sheffield, Sheffield, UK*

M. R. J. GIBBS

*Department of Metallurgy and Materials Science, University of Cambridge, Cambridge, UK*

---

The effects of cold-rolling on the atomic structure of a  $\text{Fe}_{40}\text{Ni}_{40}\text{P}_{14}\text{B}_6$  commercial metallic glass (Metglas 2826) have been investigated by X-ray and neutron diffraction. The cold-rolling is seen to produce significant changes in the structure factor  $S(Q)$  of this glass, and the changes observed are the reverse of those caused by low temperature annealing. The structure factor of the rolled specimen has also been simulated numerically. This shows that the changes in structure factor observed are consistent with a heterogeneous deformation, in which approximately 10% of the sample volume appears to have an atomic arrangement which is less well ordered than in the as-received glass. The deformation produced by rolling has finally been removed by a heat treatment whose parameters were determined with reference to a current model of structural relaxation.

---

## 1. Introduction

It is now well established that many of the physical properties of metallic glasses may be influenced by their atomic structure, and in particular that small structural rearrangements can have a significant influence on these properties. A particularly important example is provided by the changes in magnetic properties of ferromagnetic metallic glasses, which can result from low-temperature annealing, or from cold-rolling metallic glass ribbons [1-4]. One important aspect of cold-rolling is that it produces an inhomogeneous deformation in which a relatively small proportion of deformed material is found within a matrix of undeformed glass, and this can have important consequences for the interpretation of the experimental data [5].

Direct observations of the changes in structure of metallic glasses, which result from cold-rolling, have been made by X-ray diffraction experiments [6-8] and by electron diffraction [9]. However as

the changes produced are relatively small and difficult to observe, no detailed interpretation has yet been made of these data. We have been able to show in earlier measurements on an FeB glass, that the structure factor obtained in *neutron* diffraction can be quite sensitive to the small changes in structure produced by annealing [10]. It appeared worth while therefore to extend these neutron measurements to the case of cold-rolled metallic glasses, and to use the large-volume samples which this technique allows. In the present work the effects of cold-rolling on the structure of an  $\text{Fe}_{40}\text{Ni}_{40}\text{P}_{14}\text{B}_6$  (Metglas 2826) sample have been investigated using X-ray and neutron diffraction. A brief account of this work has been presented by Guoan *et al.* [11], and the present paper concerns a fuller description of both the experimental work; the details of the numerical simulations performed in order to obtain information about the heterogeneous deformation; and the heat treatment used to return the specimens to their as-received state.

\*Permanent address: Institute for Reactor Engineering Research and Design, PO Box 291-106, Chengdu, Sichuan, China.

## 2. Sample preparation

The metallic glass  $\text{Fe}_{40}\text{Ni}_{40}\text{P}_{14}\text{B}_6$  (Metglas 2826) produced by the Allied Chemical Corporation was chosen as a sample material. Normally such multi-component glasses do not make suitable candidates for diffraction experiments, but as this glass ribbon was relatively thick ( $65\ \mu\text{m}$ ) and wide ( $1.67\ \text{mm}$ ) this meant that the large volume of material needed for the neutron diffraction experiments ( $\sim 1.5\ \text{cm}^3$ ) was contained in a significant, but not unreasonable ribbon length ( $\sim 14\ \text{m}$ ). This was helpful from the point of view of the rolling treatment. The metallic glass specimen was in fact first examined in the as-received state using both X-ray and neutron radiations and then the material cold-rolled and the diffraction experiments immediately repeated.

The cold-rolling was performed using the cluster (Sendzimer) mill described by Gibbs and Evetts [12]. This mill employs work rollers of molybdenum tool steel which makes it possible to obtain reductions in ribbon thickness of up to 55%. The mill was designed to be driven mounted on a lathe and this assisted the rolling of this relatively long ribbon specimen. However, despite this mechanical aid it was found that the rolling did not produce a geometrically perfect specimen. There was curvature of the ribbon at some points, while spikes or ears of sheared material were produced at places on the edges of the ribbon. Such effects are consistent with the fact that such commercially produced ribbons do not usually have a uniform cross-section (see [12], Fig. 3). The ribbon was also found to embrittle on rolling, so that the rolled specimen often broke and was not a continuous length. This embrittlement probably arises from the cracks in the edges of the material, rather than from some change in the microstructure. As a result of this it was not practical to consider a second rolling of the whole specimen length to increase the deformation, and measurements of the thickness before ( $65\ \mu\text{m}$ ) and after the first rolling ( $54\ \mu\text{m}$ ) showed that a 17% reduction had been achieved in a single pass. The preparation of the diffraction specimens followed our usual methods. The sample for X-ray diffraction was made by winding the ribbon on a conventional aluminium flat-plate holder, with adequate spacer shims added to the clamped part of the plate to allow for the finite thickness of the wound specimen [13]. The neutron samples were made by winding ribbon on to one of the special

flat plate holders described by us in detail elsewhere [14]. The brittleness of the rolled ribbon prevented the same techniques being used, and so short lengths of ribbon were stuck to the appropriate X-ray specimen mount and a slight modified neutron specimen mount used to accommodate the whole ribbon cut into short lengths. Care was taken to make compact X-ray and neutron specimens which were geometrically as similar as possible in the as-received and rolled states.

## 3. Experimental measurements and data analysis

The X-ray experiments were performed using a Philips PW 1050 vertical diffractometer in conjunction with a molybdenum target and a (graphite) curved crystal monochromator. A range of scattering angles  $5^\circ < 2\theta < 160^\circ$  was covered in  $0.5^\circ$  steps with a pre-set time of 200 sec per step, a total scan time of 17 h. The data were processed using an extensively modified version of a computer program supplied by Wagner [15]. The structure factors  $S(Q)$  obtained for the quenched and rolled specimens are shown in Fig. 1. The neutron diffraction experiments were made with the 10H diffractometer, Dido Reactor AERE Harwell, which has three neutron detectors, and operates with an incident wavelength of 0.1 nm. A magnetic field of 1 kG was applied to the sample in a continuous magnetic circuit with no demagnetizing fields. This field was applied in the  $\mathbf{H} \parallel \mathbf{Q}$  configuration which is required to suppress the magnetic neutron scattering in this kind of experiment [14]. A range of scattering angles  $10.5 < 2\theta < 124.5^\circ$  was covered in a  $\theta:2\theta$  mode with a step length of  $0.2^\circ$ , using a pre-set count monitor. The total scan time was 22 h, and the scans were repeated three times for quenched and rolled specimens. The neutron data were analysed using our own programs and the normalization made by the self-consistent  $I(\infty)$ ,  $I(0)$  method [16] after appropriate corrections. The structure factors obtained are shown in Fig. 2, and it was estimated that the total error including experimental effects and analysis was of the order of 2%.

## 4. Structural changes observed as a result of cold-rolling

It can be seen from Figs. 1 and 2 that the  $S(Q)$  curves obtained with the two radiations are rather similar, allowing for the lower value of  $Q_{\text{max}}$  for

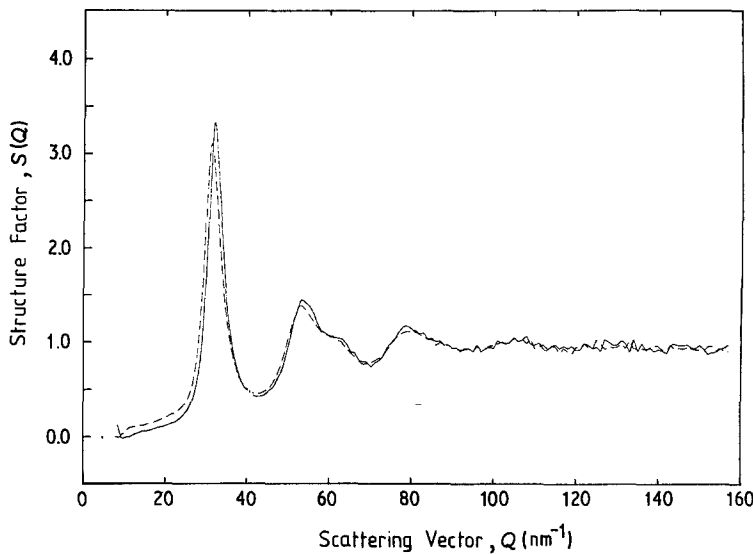


Figure 1 Structure factor curves for Metglas 2826 obtained using  $\text{MoK}\alpha$  X-radiation. The solid line is for the specimen as-received and the dashed line for the same material after cold-rolling.

the neutron curves, and this similarity can be understood if the glass  $\text{Fe}_{40}\text{Ni}_{40}\text{P}_{14}\text{B}_6$  is considered to be a pseudo-binary alloy of transition metal T, (Fe, Ni) and metalloid M (P, B). In this case the weighting terms for the partial structure factors [17] are found to be similar for X-rays and neutrons.

$$S_x(Q) = 0.810S_{\text{TT}}(Q) + 0.180S_{\text{TM}}(Q) + 0.010S_{\text{MM}}(Q) \quad (1)$$

strictly at  $Q = 0$

and

$$S_N(Q) = 0.777S_{\text{TT}}(Q) + 0.209S_{\text{TM}}(Q) + 0.014S_{\text{MM}}(Q) \quad (2)$$

The result of this is that  $S_x(Q)$  and  $S_N(Q)$  will be alike, and this is generally the case with transition metal-metalloid glasses (except for cobalt-based glasses because cobalt has a low value of the nuclear scattering length). Thus, as in the case of the FeB glass examined in our annealing work [10] the neutron method does not provide any special improved visibility between the alloy components, but rather the two radiations (neutrons and X-rays) provide mutual confirmation of the changes in  $S(Q)$  observed. A second and somewhat related point is that the information obtained from the Fourier transform of the total  $S(Q)$  in the case of a metallic glass like Metglas 2826 is essentially information about the topological arrangements of the atoms. The conditions which are necessary to allow the chemical arrangements of the constituent atoms to be studied are not fulfilled in this case [18]. The disorder and the structural arrangements which are being studied, are therefore topological, and this means for example that the results from simple one-component model systems can be used in order to try and understand the nature of these topological changes.

A comparison of the curves in Figs. 1 and 2 allows the following observations to be made. The structure factors of the as-quenched specimens show the characteristic features common to most metallic glasses, namely a sharp first peak, second peak with shoulder on the high  $Q$  side and well

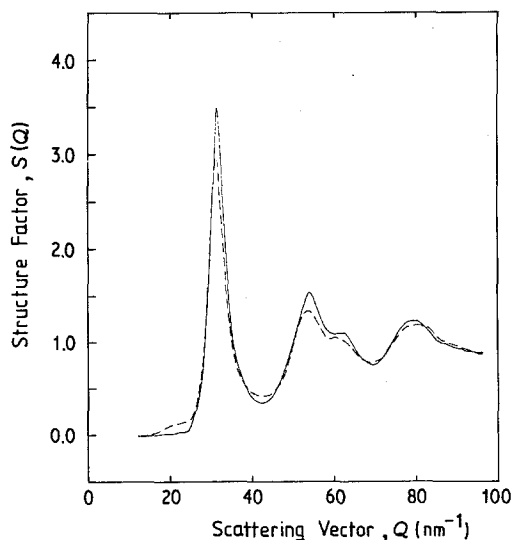


Figure 2 Structure factor curves for Metglas 2826 obtained using thermal neutrons of  $\lambda = 0.1$  nm. The solid line is for the specimen as-received and the dashed line for the same material after cold-rolling.

TABLE I The positions of peaks in the structure factors of as-received and cold-rolled Metglas 2826,  $Q_1$ ,  $Q_2$  etc are given with corresponding peak positions in the reduced RDFs,  $r_1$ ,  $r_2$  etc. The second peak shoulder is described by  $2s$ . The heights of the first peak in  $S(Q)$ ,  $S(Q_1)$  is also given and the coordination number  $n_1$  from the RDF.

Sample state	Radiation	Peak height and positions in $S(Q)$ in nm					Radial distances in the reduced RDF in nm and the coordination number from the RDF				
		$Q_1$	$Q_2$	$Q_{2s}$	$Q_3$	$S(Q_1)$	$r_1$	$r_2$	$r_{2s}$	$r_3$	$n_1$
As-received	X-ray	0.315	0.530	–	0.787	0.340	0.262	0.430	0.491	0.634	11.4
	Neutron	0.312	0.538	0.620	0.790	0.348	0.257	0.434	–	0.639	11.5
Cold-rolled	X-ray	0.310	0.533	–	0.790	0.309	0.257	0.430	–	0.636	11.2
	Neutron	0.310	0.535	–	0.800	0.304	0.254	0.434	–	0.642	11.3

developed oscillations out to  $Q_{\max}$ . The structure factor of the rolled sample shows the same basic features but the height of the first peak is noticeably reduced, of order 10% and also its position is shifted slightly to lower  $Q$  value. The subsequent peaks in  $S(Q)$  are also reduced by a smaller proportion, and their position in  $Q$  remains roughly unchanged, while the second peak shoulder becomes less distinct. The form of  $S(Q)$  at the onset of the first maximum is also altered. A numerical description of these changes is given in Table I. In general the changes in peak height are larger than those which have been observed by diffraction experiments elsewhere, although there is not in fact a clear picture of the likely magnitude of the changes, which must depend on factors such as the elastic moduli, hardness and packing density and thermomechanical history of the glass involved.

For example, in an early demonstration of the effects of cold-rolling on metallic glass structure [6] showed that when a  $\text{Pd}_{80}\text{Si}_{20}$  glass was deformed by 20% and by 40%, the height of the first peak in the diffracted *intensity distribution*  $I(Q)$  was reduced by 4% and 6% respectively. In a later study on a similar  $\text{Pd}_{80}\text{Si}_{20}$  glass it was found that a 20% deformation produced no change in the height of the first peak in the *structure factor* and a 40% deformation produced a 4% reduction in this peak height [9]. Very small changes in  $S(Q)$  were also observed [8] for the case of a  $\text{Pd}_{80}\text{Si}_{20}$  specimen, 20% cold-rolled after annealing, while a greater deformation of 35% was found to reduce the first maximum in  $S(Q)$  by only 1%. In contrast very much greater changes ( $\sim 40\%$ ) in the intensity profile  $I(Q)$  were observed [9], when making *selected area* electron diffraction measurements on the deformed regions in an  $\text{Ni}_{75}\text{B}_{17}\text{Si}_8$  specimen. It appears that the changes observed in our present

study lie between the limits of the changes observed elsewhere, while the excellent agreement between our two sets of data obtained with different radiations provides independent confirmation of these somewhat larger changes in  $S(Q)$ .

An equally important point is that the origin of the differences between these results referred to above may lie, either wholly or partly, in the different thermomechanical histories of the specimens concerned. The degree of structural relaxation at any time is a complex function of thermomechanical history [19, 20], and the state of relaxation will govern the ease of mechanically activated motion. Although the *precise* history of the present sample material is not known, it had an anneal for at least  $10^8$  sec at 300 K, between the initial glass-forming process and the start of these experiments. Thus according to Equation 11 as given in [20], all those atomic rearrangements having values of activation energy,  $E$ , less than 1.25 eV have already given their contributions to changes in  $S(Q)$ . The structure factor measured initially was therefore characteristic of the as-received, rather than the as-quenched material. Furthermore a period of approximately  $6 \times 10^4$  sec elapsed between the cold-rolling and the second set of neutron experiments. Thus any structural changes brought about by the cold-rolling, which had activation energies  $E$  less than 1.06 eV for thermally induced relaxation would have been activated before the second set of diffraction measurements. Hence the changes in  $S(Q)$  which are seen after cold-rolling reflect not only the cold-rolling process, but also the thermal history up to the time of the measurements. This may be one source of apparent discrepancy between sets of data obtained under different circumstances in different laboratories described above.

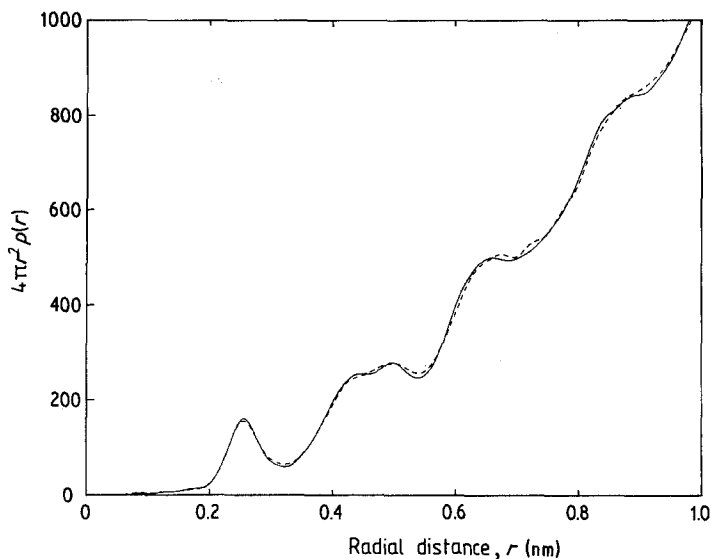


Figure 3 The radial distribution function curves obtained from X-ray data on Metglas 2826 which has an atomic density of  $84.1 \text{ atoms nm}^{-3}$ . The solid line is for the specimen as-received, and the dashed line for the same material after cold-rolling.

The changes of structure, in real space, as expressed by the appropriate curves, are of a rather similar nature to the changes in  $S(Q)$ . The rolling treatment is seen to cause a slight reduction in the magnitude of the oscillations in the RDF. This is illustrated by means of the X-ray data, in Fig. 3. The neutron curves are similar, with slightly lower resolution on account of the smaller value of  $Q_{\text{max}}$ . Table I gives some numerical values of parameters from  $G(r)$  and the RDF and shows that the changes in  $S(Q)$  do not result in very large differences in the values of either the radial atomic distances or the coordination number.

One interesting point is that the cold-rolling appears to have exactly the opposite effect on the structure to that produced by low temperature annealing. Both X-ray [21] and neutron diffraction experiments [10] show that annealing produces an increase in the peak heights, and a general sharpening of the features in  $S(Q)$ .

### 5. Models, and simulation of structural deformation

In view of the influence of deformation on the physical properties of metallic glasses it is not surprising that several authors have discussed the possible mechanisms of this deformation. Often crystalline defects have been used as a starting point, and to a certain extent an amorphous solid can be considered to be a material with an extremely high density of dislocations. Since defects can be defined — as for example in a continuous medium, without recourse to a crystalline

lattice there is no fundamental problem over their definition in amorphous solids. Chaudhari [22] for example, has suggested that the effects of deformation can be qualitatively associated with the presence of screw dislocations alone, and that at low temperatures deformation occurs primarily through the motion of dislocations. A common feature of several of these kind of models is that they imply the structure defect is not a vacancy-like defect, and some experimental evidence for this is provided by positron annihilation experiments on cold-rolled metallic glasses [23]. On the other hand, by using the ideas of viscous flow in the liquid state and extrapolating to amorphous materials, it was suggested [24] that the structural defects are individual sites where the preferred short range order is perturbed, and that since the viscosity is related to the defect concentration, viscosity will be reduced in slip-band regions during deformation. A rather different approach to structural defects is provided by the recent work of Egami *et al.* [25] in which defects are defined in terms of the distribution of internal stresses, and local symmetry. Computer simulation suggests that motion of dislocation-like, vacancy-like, and interstitial defects can all occur during plastic deformation. Motion of vacancy-like defects is also a feature of earlier computer simulation [26], which shows the chain collapse of holes which results in step nucleation and propagation on a macroscopic scale.

Whilst it is clear that it is not possible to decide which of these models is appropriate from our dif-

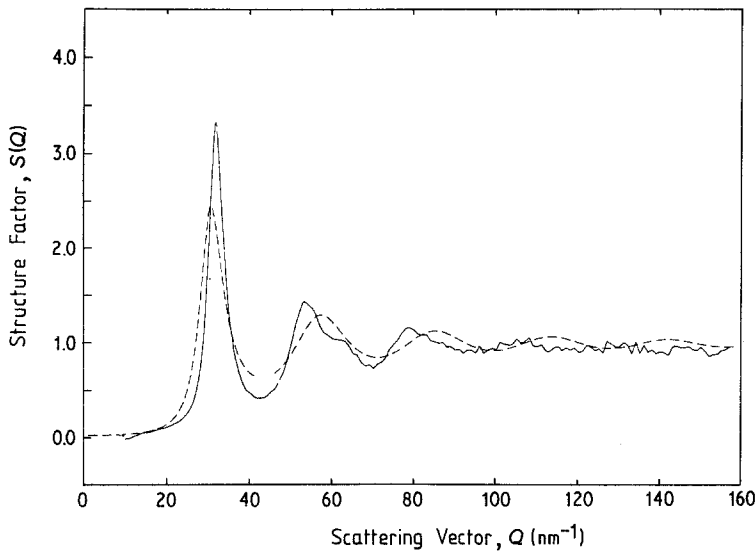


Figure 4 The experimental  $S(Q)$  curve for the as-received Metglas 2826 derived from X-ray diffraction is shown by the solid line. The calculated  $S(Q)$  curve based on the hard-sphere model of a liquid metal discussed in the text, is shown by the dotted line.

fraction data alone, not least for the fact that diffraction data represent a volume average over the whole specimen, while it is agreed that inhomogeneous deformation is highly localized. Nevertheless the structure factor curves do contain information about modifications to the atomic scale structure induced by rolling. A common feature to most of these models is this idea of an inhomogeneous deformation in which a high level of defects is concentrated in the deformed regions which have reasonably well defined boundaries. To a first approximation, if we assume that a fairly uniform deformation can be associated with some regions (which may extend beyond the observable shear bands), then the structure factor of rolled material might be represented in a simple additive way.

$$S(Q)_{\text{rolled}} = (1 - V)S(Q)_{\text{as-quenched}} + VS(Q)_{\text{deformed}} \quad (3)$$

where  $V$  is the volume proportion of the deformed material in the specimen. If the structure factor  $S(Q)_{\text{deformed}}$  could be measured with any precision then the factor  $V$  could be evaluated. Alternatively either one or both of the structure factors on the right-hand side of Equation 3 can be simulated, in order to obtain some reasonable estimate of  $V$ .

In order to choose a suitable form for  $S(Q)_{\text{deformed}}$  it is necessary to make some deductions about the possible atomic arrangements in the deformed region. First it is clear that both deformed regions and matrix are truly amorphous, and that as under-cooled liquids, the geometrical

arrangements of atoms in both cases must bear some resemblance to that of the liquid state. In fact the structural similarities (and the differences) between the same metal alloys in both liquid and glassy states were systematically investigated in many diffraction measurements; see for example [27]. These differences, and particularly the loss of detail in  $S(Q)$  in the liquid are similar to the variations in  $S(Q)$  produced here by rolling. A possible reason for this is that the application of a load to a metallic glass causes a significant reduction in viscosity within the shear bands while the removal of the load, on exit from the work rollers, is accompanied by a rapid increase in viscosity. This sudden increase in viscosity is analogous to the increase which takes place during the initial vitrification of the glass, and suggests that whilst melt-spinning represents a thermal quenching, cold-rolling produces an effective "pressure quench". Whilst both of these quenching processes lead to "liquid-like" structures, the implication is that the pressure quench gives a more disordered atomic arrangement in these deformed regions.

In the absence of structural data on the Metglas 2826 specimen in the liquid state, we chose first to simulate  $S(Q)_{\text{deformed}}$  by using a calculated curve, namely a hard-sphere simulation for liquid metals [28], as modified by Greenfield *et al.* [29]. It is possible that this curve could overestimate the disorder in the deformed regions, but this could compensate for having a sharp boundary between deformed and undeformed parts of the specimen.

The calculated curve based on this hard-sphere model is shown in Fig. 4, together with the experi-

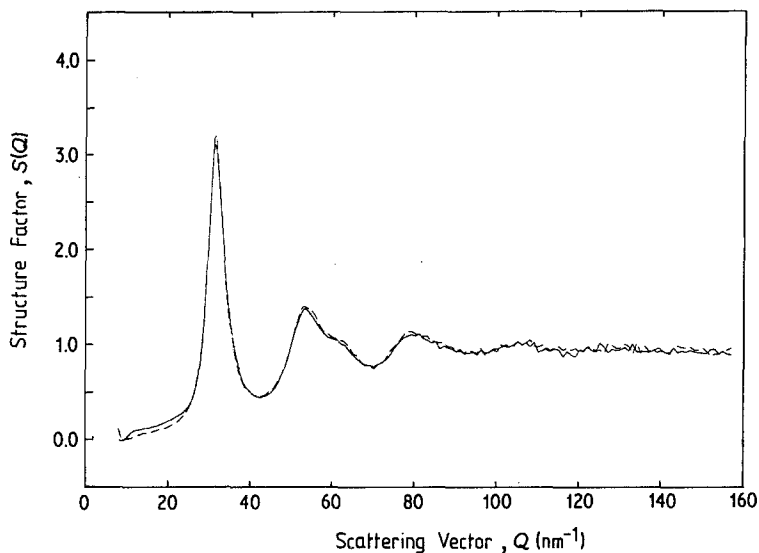


Figure 5 The result of the simulation of the structure factor curve for the cold-rolled Metglas 2826 is shown. The solid line is the experimental result from X-ray diffraction, and the dashed line the simulated  $S(Q)$  curve.

mental  $S(Q)$  for the as-received specimen. The calculated curve has been based on a hard-sphere diameter  $\sigma = 0.222$  nm, and a packing fraction  $\eta = 0.445$ , and these values were chosen in order to match closely with the experimental curve for values of  $Q$  between 0 and  $\sim 70$  nm $^{-1}$ . It may be noted that this hard-sphere diameter is significantly smaller than the Goldschmidt diameter of the real atoms iron and nickel, and this appears to be a normal feature of this kind of simulation [29].

The result of fitting the structure factor of the rolled sample is shown in Fig. 5, in which the calculated curve has a value of  $V = 0.14$ , that is 14% of the deformed  $S(Q)$ , and 86% as-received  $S(Q)$ . The agreement between the experimental and simulated curves is very good, except perhaps at small  $Q$  values, and the average difference between the curves is less than 3%, which is commensurate with the experimental uncertainty.

In order to establish that this result did not depend too sensitively on the structure factor chosen for the deformed regions, it was decided to make a second simulation based on experimental data rather than a model calculation. Ideally a structure factor curve for liquid Metglas 2826 should be used, but as this was not available it was decided to produce a curve by modifying the structure factor curve of another similar alloy for which such data exists, according to the following considerations. There are of course two coordinates for any structure factor  $Q, S(Q)$  which might be independently scaled in various ways. We will consider the ordinate,  $Q$ , first. The position of

the first peak in  $S(Q)$  reflects very accurately the first neighbour distance in real space  $r$ , and hence from a knowledge of the average Goldschmidt diameter of the transition metal atoms, it is possible to deduce the likely position of the first peak in  $S(Q)$ . In addition the positions of the subsequent peaks are also quite well defined because the ratios of the positions of the first/second and second/third peaks are well described by predictable numbers. These are characteristically different for the liquid and glassy states [27], but vary little for glasses of the same kind (e.g. transition metal-metalloid types). In addition we have found independently, from measurements on transition metal glasses, which can be made over wide composition ranges, that these interpeak ratios hold reasonably fixed out to even the fifth or sixth maxima in  $S(Q)$ . Thus if a simple linear scaling is made in  $Q$ , in order to bring the first maximum to a desired position, then the subsequent maxima will also occur in predictable positions. For the case of the abscissa it is known that the amplitude of the oscillations in  $S(Q)$ , about unity, are determined mainly by the packing density of the material. In general a predictable reduction in the amplitude of these oscillations occurs in going from the glassy to liquid states. In order to produce a structure factor curve for molten Metglas 2826 we have therefore used our own data for 2826 glass, together with the published curves for liquid and glassy  $\text{Fe}_{80}\text{P}_{13}\text{C}_7$  [30] and made a simple linear scaling of  $Q$ , and  $S(Q)$  (i.e.  $|S(Q) - 1|$ ) axes. A thorough search of the literature has suggested that the  $\text{Fe}_{80}\text{P}_{13}\text{C}_7$  alloy is the most appropriate

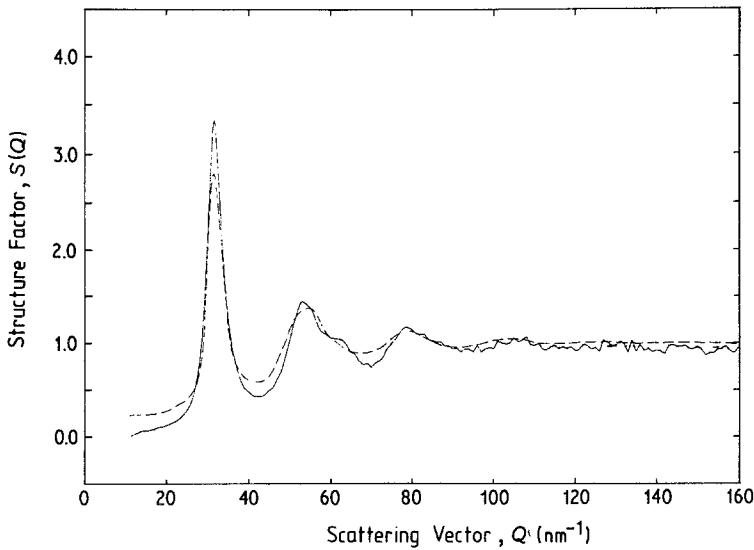


Figure 6 The experimental  $S(Q)$  for the as-received Metglas 2826 is shown by the solid line, and the curve produced from data on  $\text{Fe}_{80}\text{P}_{13}\text{C}_7$  shown by the dotted line.

candidate for this process. Fig. 6 shows the experimental  $S(Q)$  curve for the as-received Metglas 2826, together with the curve we have produced for "liquid 2826". These curves may be compared with the original data for  $\text{Fe}_{80}\text{P}_{13}\text{C}_7$  (Fig. 1 in [30]). The result of a simulation of the structure factor of the cold-rolled Metglas 2826 based on the curves given in Fig. 6, is shown in Fig. 7. It is interesting to note that the overall agreement is less good than when the hard-sphere liquid model was used, Fig. 5, but that the volume fraction of disordered material is less, 8% as opposed to 14%. We conclude therefore that a likely value of the deformed volume may be close to the mean of these two figures, say around 10%.

There are relatively few other determinations of

the disordered volume fraction with which comparison of the present value can be made. An estimate of the deformed volume  $V$  can be made from the electron microscope examination of an  $\text{N}_{75}\text{B}_{17}\text{Si}_8$  glass [9], although this estimate is subject to the qualification that shear bands in ribbon specimens and thin films may be different in character [31]. An electron micrograph (Fig. 7 in [9]) shows bright bands associated with the disordered regions which occupy of the order of 19% of the area of the micrographs of that thin film. The selected area diffraction patterns of this specimen which have already been referred to above show that when the disordered region *alone* was examined the first peak in the intensity distribution was reduced by about 40%. This figure

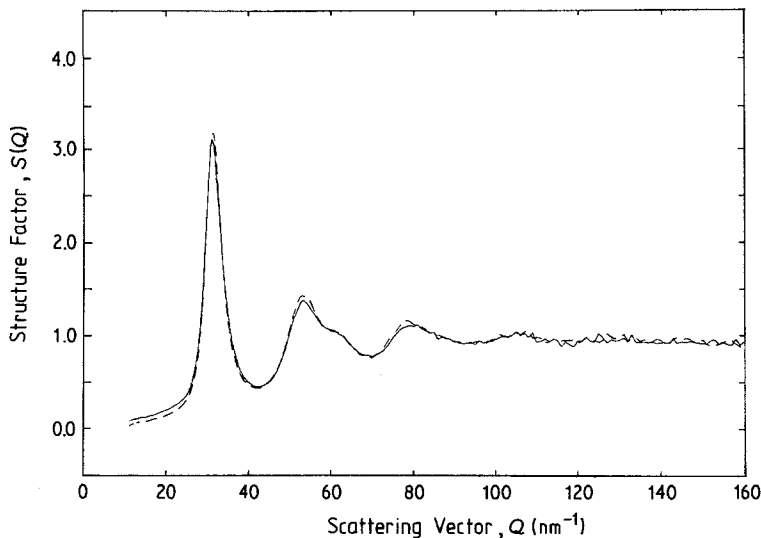


Figure 7 The result of the second simulation of the structure factor of the cold-rolled Metglas 2826 is shown, with the curves identified as in Fig. 5.



implies that if the disordered region occupied approximately 10% of the total volume, then the decrease in the first peak in  $I(Q)$  when the whole sample was irradiated would be around 6%, which is commensurate with the 10% change in  $S(Q)$  observed in our present study.

A further and perhaps more appropriate comparison can be made with the more detailed observations of shear bands which have been made by electron microscopy [31]. Donovan and Stobbs have examined shear bands in both  $\text{Ni}_{76}\text{P}_{24}$  and  $\text{Fe}_{40}\text{Ni}_{40}\text{B}_{20}$  metallic glasses. The NiP specimens which were produced by electro-deposition were deformed as free films on their microscope grids and also when still attached to brass substrates. In the first case shear bands of thickness 20 nm and having characteristic separation of  $2\ \mu\text{m}$  were observed. This gives a volume fraction of material in the shear band of 1%. In the latter case shear bands with thickness between 40 to 60 nm and separation between 0.2 to  $1.0\ \mu\text{m}$  were observed, giving a larger volume fraction 8.5%. The  $\text{Ni}_{40}\text{Fe}_{40}\text{B}_{20}$  (Vitrovac E0040, a commercial sample not unlike Metglas 2826) was supplied as fast-quenched ribbon, and deformed in bulk and thinned by electropolishing. Shear bands having thickness 10 to 20 nm and spacing  $1\ \mu\text{m}$  were observed, which when aligned at 45% to the ribbon, as in the present case, gives a volume fraction of 2%.

These estimates are of the volume fraction of material within the electron microscope image of the shear bands. There is in fact some reason to believe that these regions are associated with the highest levels of stress, while the disordered volume measured in the diffraction experiments may extend over larger regions. Evidence for the first of these assertions comes from measurements of the variation of magnetic properties produced by cold-rolling [4]. Calculation shows that the dramatic changes in coercive force observed can be accounted for if a relatively small volume, 1.5%, is associated with the highest levels of stress (close to yield strength, where close-packed regions may approach the theoretical strength). This volume fraction is essentially the same as that attributed to the shear bands, as obtained above. On the other hand evidence for the existence of strain fields which may atomically disorder the material beyond the shear band boundaries is provided by the observations of the interactions of shear bands (Fig. 12 in [31]), which shows relative displace-

ments ( $0.03\ \mu\text{m}$ ) of the order of twice the shear-band width (10 to 20 nm). A somewhat related point is that there is also evidence [31, 32] that structural alteration can be retained even after removal of the shear band itself.

The conclusions deduced from these simulations are therefore that the diffraction measurements and the changes in structure factor observed are consistent with the cold-rolled material having a fraction of disordered material ( $\sim 10\%$ ), and that this value is within a factor of 5 of the volume of the shear-band regions (2%) as deduced by direct observation. In addition the variations in the atomic scale structure produced by the cold-rolling, and which can be characterized by a kind of "pressure quenching" mechanism are consistent with an increased disorder in which there is a more liquid-like arrangement of atoms.

## 6. Annealing treatment for the relief of deformation

In addition to the analysis of the effects of cold-rolling the present measurements have also permitted an investigation of the possible reversibility of these structural changes to be made. In this context it is generally understood that structural relaxation and deformation are manifestations of the metastability of metallic glasses for which several metastable glassy structures may be separated from one another by various energy barriers. Structural re-arrangements which still preserve the glassy state occur through the activation of different processes, possibly the motions of individual atoms or groups of atoms – but which have not as yet been unequivocally identified. The annealing of the cold-rolled specimen provides an opportunity of illustrating the general point that cold-rolling has a "disordering effect" and annealing an "ordering effect" on metallic glass structure, but more specifically because the processes of structural change are conveniently described in terms of statistical thermodynamic models, an appropriate choice of heat treatment can provide independent confirmation of "log–time" kinetics, and the underlying principles of the relaxation model based on a spectrum of activation energies [20].

The overall schedule for the present experiments has been largely determined by the availability of the neutron diffraction instrument, which was arranged in the usual way within the SERC/UKAEA neutron beam programme. Thus

TABLE II Thermo-mechanical history of the Metglas 2826 material from which the diffraction specimens were made.

Schedule of events	Time intervals at $\sim 300$ K
Original melt spinning	$> 10^8$ sec
Diffraction experiments: as-received	
*Cold rolling treatment 17% reduction	$2.6 \times 10^5$ sec
Diffraction experiments: cold rolled	$4.5 \times 10^5$ sec
*Heat treatment $1.1 \times 10^4$ sec at 573 K	$4.0 \times 10^7$ sec
Diffraction experiments: annealed	$4.5 \times 10^6$ sec

several months after the initial neutron experiments on the as-received and cold-rolled specimens an opportunity arose to measure the same sample in a relaxed (annealed) state. It was deduced at that time, that a heat treatment of approximately 3 h at  $300^\circ\text{C}$  would be appropriate to return the sample to its as-received state. The full specification of the thermomechanical history of the Metglas specimens up to the time of these final diffraction experiments is given in Table II. This is the first time, as we are aware, that such a specification has been made in a study of this kind.

The time and temperature of the heat treatment were based on the assumption that the cold-rolling had created processes having small activation energies [33]; that processes having energies of less than 1.23 eV would have been annealed out in the  $4 \times 10^7$  sec period of storage at room temperature, and that processes with energies  $E < 1.94$  eV were removed in the  $300^\circ\text{C}$  anneal ( $1.1 \times 10^4$  sec).

In the event, electronic malfunctions in the neutron experiments meant that incomplete data were obtained. However the results of the X-ray experiments on the annealed specimen, which were done at the same time, (and like the neutron experiments performed and analysed in precisely the same manner as the earlier experiments described in Section 3) confirmed that the heat treatment had produced the desired result of restoring the structure of the sample towards its as-received state. This is illustrated in Fig. 8, which shows the structure factors  $S(Q)$  obtained for the as-received and post-annealed samples, both curves

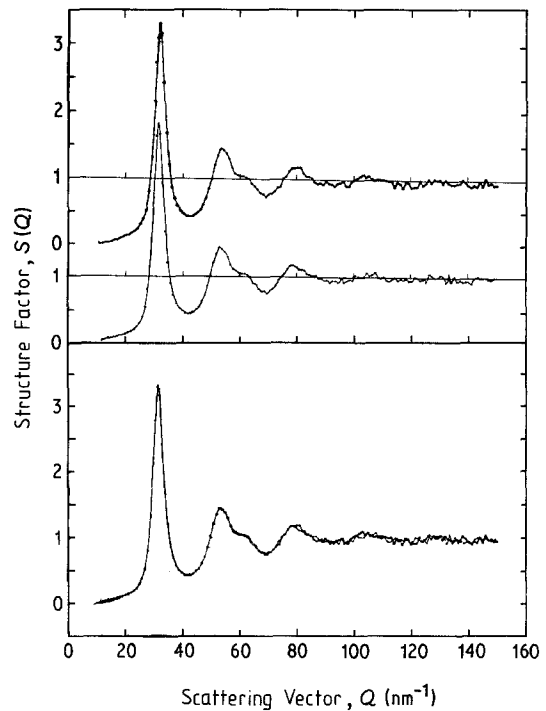


Figure 8 The structure factor  $S(Q)$  curves obtained by X-ray diffraction for the Metglas 2826 in the as-received, and heat-treated conditions are shown independently and superimposed to illustrate the extremely close similarities between the two curves.

individually and also superimposed. This superposition shows that the positions and heights of the peaks in the  $S(Q)$  curves are faithfully reproduced and that any disagreement is significantly less than the experimental uncertainty in the data points – which derive directly from the observed intensity distribution. This superposition provides a striking demonstration of both the reversibility of the structural changes induced, and the correctness of the application of “log–time” kinetics.

## 7. Conclusion

X-ray and neutron diffraction experiments have been made on a sample of  $\text{Fe}_{40}\text{Ni}_{40}\text{P}_{14}\text{B}_6$  metallic glass (Metglas 2826) in order to determine the nature of the structural changes produced by a cold-rolling treatment. Despite many detailed experimental differences between the two measurements, including such factors as significant differences in the duration of the scans (one day and three days respectively), there is good agreement between the X-ray and neutron data obtained. The cold-rolling appears to cause significant changes in the structure factor curves, which

are consistent with an increased atomic disorder. The structure factor of the rolled specimen has been successfully simulated with the aid of calculated  $S(Q)$  curves based on a hard-sphere model of a liquid metal, and also on the scaled experimental data for a similar alloy in the molten state. These simulations support the concept of an inhomogeneous deformation produced by rolling and allow an estimate to be made of the volume fraction of the disordered materials. This fraction is roughly commensurate with the volume of material in the shear band regions. A heat treatment has also been used to demonstrate the reversibility of the structural changes produced.

### Acknowledgements

Financial support from the Science and Engineering Research Council and the assistance of the University Support Group at AERE Harwell are gratefully acknowledged. The authors would like to thank Dr J. E. Evetts for his help and advice. The experiment described in this paper was suggested to the authors by Professor R. W. Cahn, during discussion of previous annealing work at the Informal Meeting on Rapidly Quenched Metals, Cambridge, 1981.

### References

1. F. E. LUBORSKY, J. L. WALTER and D. G. LEGRAND, *IEEE Trans. Mag.* **MAG-12** (1976) 930.
2. R. S. WILLIAMS and T. EGAMI, *ibid.* **MAG-12** (1976) 927.
3. M. R. J. GIBBS, J. E. EVETTS and N. J. SHAH, *J. Appl. Phys.* **50** (1979) 7642.
4. M. R. J. GIBBS, J. E. EVETTS and M. E. HORTON, *J. de Physique* **C8** (1980) 41.
5. J. E. EVETTS, in Proceedings of the 3rd International Conference on Rapidly Quenched Metals, Brighton, July 1978 (Metals Society, London, Vol. 2, 1978) p. 477.
6. T. MASUMOTO and R. MADDIN, *Mater. Sci. Eng.* **19** (1975) 1.
7. Y. WASEDA and T. MASUMOTO, *Sci. Rep. RITU* **27A** (1978) 21.
8. Y. WASEDA and T. EGAMI, *J. Mater. Sci.* **14** (1979) 1247.
9. T. MASUMOTO, H. KIMURA, A. INOUE and Y. WASEDA, *Mater. Sci. Eng.* **23** (1976) 141.
10. N. COWLAM, K. DINI and H. A. DAVIES, "Metallic Glasses: Science and Technology" (Kultura, Budapest, 1981) Vol. 1. p. 267.
11. WU GUOAN, N. COWLAM and M. R. J. GIBBS, "Structure of Non-crystalline Solids" (Taylor and Francis, London, 1983) pp. 474-84.
12. M. R. J. GIBBS and J. E. EVETTS, *Scripta Metall.* **14** (1980) 63.
13. K. DINI, N. COWLAM and H. A. DAVIES, *J. Phys. F: Met. Phys.* **12** (1982) 1553.
14. N. COWLAM, H. A. DAVIES and K. DINI, *J. Non-Cryst. Solids* **40** (1980) 377.
15. C. N. J. WAGNER, Technical Report to National Science Foundation Grant GL 3213 (1968).
16. J. E. ENDERBY, "Physics of Simple Liquids", edited by H. N. V. Temperley, J. S. Rowlinson and G. S. Rushbrooke (North Holland, Amsterdam 1968) p. 613.
17. T. E. FABER and J. M. ZIMAN, *Phil. Mag.* **11** (1965) 153.
18. M. SAKATA, N. COWLAM and H. A. DAVIES, *J. Non-Cryst. Solids* **46** (1981) 329.
19. M. R. J. GIBBS and J. E. EVETTS, in Proceedings of the 4th International Conference on Rapidly Quenched Metals, Vol. 1, Sendai, Japan, August 1981 (Japanese Society of Metals, Sendai, 1982) p. 479.
20. M. R. J. GIBBS, J. E. EVETTS and J. A. LEAKE, *J. Mater. Sci.* **18** (1983) 278.
21. T. EGAMI, *J. Appl. Phys.* **50** (1979) 1564.
22. P. CHAUDHARI, *J. de Physique* **C8** (1980) 267.
23. H. S. CHEN and S. I. CHUANG, *Appl. Phys. Lett.* **27** (1975) 316.
24. F. SPAEPEN, in Proceedings of the 3rd International Conference on Rapidly Quenched Metals, Vol. 2, Brighton, July 1978 (Metals Society, London, 1978) p. 253.
25. T. EGAMI, K. MAEDA and V. VITEK, *Phil. Mag.* **41A** (1980) 883.
26. T. MAEDA and S. TAKEUCHI, *Suppl. Sci. Rep. RITU. Sec. A* **26** (1978) 87.
27. Y. WASEDA, H. OKAZAHI and T. MASUMOTO, *J. Mater. Sci.* **12** (1977) 1927.
28. N. W. ASHCROFT and J. LEKNER, *Phys. Rev.* **145** (1966) 83.
29. A. J. GREENFIELD, N. WISER, M. R. LEENSTRA and N. VAN DER LUGT, *Physica* **59** (1972) 571.
30. Y. WASEDA and T. MASUMOTO, *Zeit Physik* **B22** (1975) 121.
31. P. E. DONOVAN and W. M. STOBBS, *Acta Metall.* **29** (1981) 1419.
32. C. A. PAMPILLO, *Scripta Metall.* **6** (1972) 915.
33. M. R. J. GIBBS, "Metallic Glasses: Science and Technology" Vol. 2 (Kultura, Budapest, 1981) p. 37.

Received 31 May  
and accepted 15 August 1983